Electronic Supplementary Material (ESI) for Lab on a Chip.

Enhanced acoustic streaming effects via sharp-edged 3D microstructures

William S. Harley[1,2], Kirill Kolesnik[1], Daniel E. Heath[1], David J. Collins[1,3]
[1]Department of Biomedical Engineering, University of Melbourne, Melbourne, VIC 3010, Australia
[2]Micro Nano Research Facility, RMIT University, Melbourne, Victoria 3000, Australia
[3]The Graeme Clark Institute, The University of Melbourne, Parkville, VIC, 3010, Australia

Corresponding author: david.collins@unimelb.edu.au

Supplementary Note 1
Sharp edge height calculation

The sharp edge height can be estimated from the geometrical parameters of the pillar structure, such as pillar width $w = 30\mu m$ and sharpness angle α (Fig. S1a). Since the shape of the pillar is diverging from a simple wedge, the height of the edge is parametrized as shown in Fig. S1b-e. The expression for the height a can be derived as follows:

$$a = \frac{w}{2\sqrt{\left(1 - tan\left[\frac{\pi}{4} - \frac{\alpha}{2}\right]\right)^2 + 1}}. \quad \text{(S1)}$$

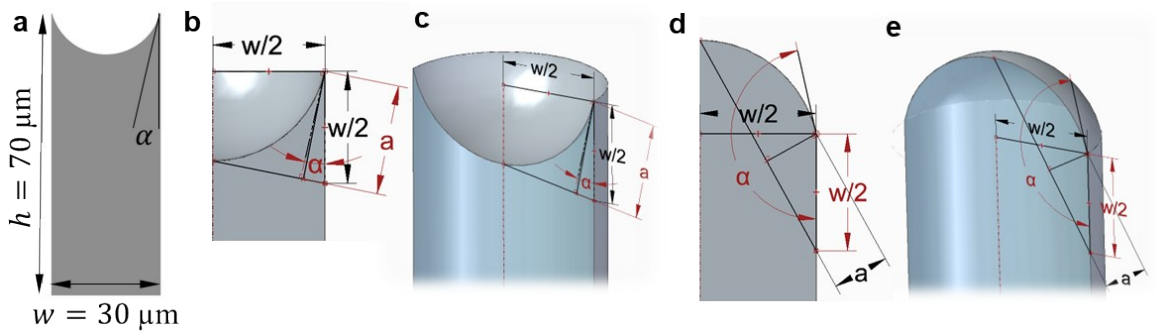

Fig. S1. Sharp edge structure. (a) Pillar size and the sharp edge angle. (b-e) The height a estimation for concave (b,c) and convex (d,e) shapes.

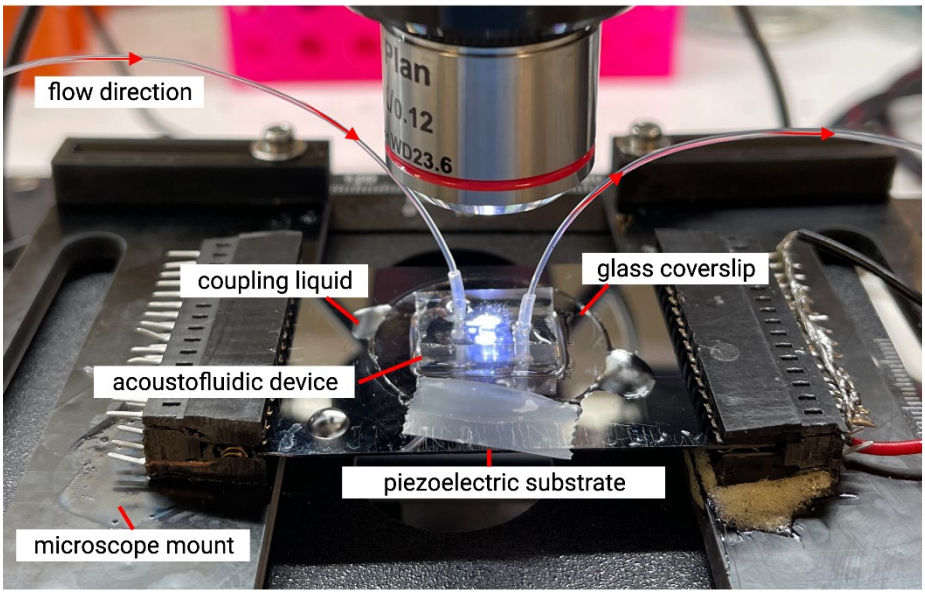

Fig. S2. Experimental setup for exploring particle manipulation within a microfluidic device, comprising a microfluidic channel coupled to a piezoelectric transducer through a water layer, with particle suspensions introduced by a syringe pump and observed using a fluorescence microscope.

Supplementary Note 2
Governing equations

Perturbation theory was used to model the system with harmonic actuation. The perturbation approach has been previously validated for studying vibrating structures with sharp edges, and it has shown agreement with both the transient modeling and experimental results[56]. Physical fields can be decomposed into initial, first and second-order terms $g = g_0 + g_1 + g_2$ where 0-term is the initial background state. First-order fields are harmonic with $g_1(r,t) = \bar{g}_1(r)e^{i\omega t}$, where $\bar{g}_1(r)$ is the complex-valued amplitude, $\omega = 2\pi f$ is the angular frequency, and f is the oscillation frequency.

In the first step, we solve the first-order (linear) equations, leaving out the common time-dependent factor. Reintroducing the phase factor $e^{i\omega t}$, the time-dependent solution can be obtained. The PDMS and commercial IP-Dip material (printed component) domains are modeled with the solid mechanics module in COMSOL. In the Voigt representation the substrate mechanical stress tensor σ_1 and the elastic displacement field u_1 are coupled with Hooke's Law. For isotropic elastic materials, this is given by

$$\begin{pmatrix}\sigma_r\\ \sigma_z\\ \sigma_\theta\\ \sigma_{rz}\end{pmatrix} = \begin{pmatrix}C_{11} & C_{12} & 0 & 0\\ C_{12} & C_{11} & 0 & 0\\ 0 & 0 & C_{11} & 0\\ 0 & 0 & 0 & C_{44}\end{pmatrix}\begin{pmatrix}\partial_r u_r\\ \partial_z u_z\\ u_r/r\\ \partial_z u_r + \partial_r u_z\end{pmatrix}, \tag{S2}$$

where C_{ij} are the elastic constants. We introduce damping in the system through complex-valued elastic coefficients[57]

$$C_{ij} = C_{ij}^{'} + iC_{ij}^{''} = C_{ij}^{'}(1 + i\eta), \tag{S3}$$

where η is an isotropic loss factor. The Cauchy equation takes the form

$$\nabla \cdot \sigma_1 = -\rho_0\omega^2 u_1, \tag{S4}$$

where ρ_0 is the mass density. The storage modulus $C_{ij}^{'}$ can be defined through the longitudinal c_L and transverse c_T sound speeds or Young's modulus E and the Poisson's ratio ν

$$C_{11}^{'} = c_L^2\rho_0 = \frac{E(1-\nu)}{(1+\nu)(1-2\nu)}, \tag{S5}$$

$$C_{44}^{'} = c_T^2\rho_0 = \frac{E}{(1+\nu)}, \tag{S6}$$

$$C_{12}^{'} = C_{11}^{'} - 2C_{44}^{'}. \tag{S7}$$

A roller boundary condition is applied on all side walls, with

$$u_1 \cdot n = 0, \tag{S8}$$

where n is the normal to the boundary vector. We use a PML on the top wall to set a non-reflecting boundary as shown in Fig. S3a. The PML acts as an artificial absorbing domain by imposing a complex-valued coordinate displacement in the z-direction (polynomial stretching)

$$\Delta z = \lambda\hat{z}(1-i) - h_{PML}\hat{z}, \tag{S9}$$

where λ is the acoustic wavelength, and $\hat{z}$ is a local dimensionless coordinate which varies from 0 to 1 over the PML height $h_{PML} = \lambda/2$.

In the fluid domain, governing equations of continuity, energy, and momentum conservation are considered, with

$$\frac{\partial \rho_1}{\partial t} = -\rho_0 \nabla \cdot v_1, \tag{S10}$$

$$\frac{\partial T_1}{\partial t} = \nabla\left(D_T \nabla T_1\right) + \frac{\alpha_T T_0 \, \partial \rho_1}{\rho_{0,w} C_p \, \partial t}, \tag{S11}$$

$$\rho_{0,w}\frac{\partial v_1}{\partial t} = -\nabla p_1 + \beta\mu\nabla\left(\nabla \cdot v_1\right) + \mu\nabla^2 v_1, \tag{S12}$$

where v_1 is fluid velocity perturbation, ρ_1 is density perturbation, T_1 is temperature perturbation, D_T is the thermal diffusivity of the liquid, α_T is the isobaric thermal expansion coefficient relating density change with temperature, $\rho_{0,w}$ is the zeroth-order density of the fluid at rest and C_p is the specific heat capacity at constant pressure, p_1 is the pressure perturbation, β is the viscosity ratio, relating the bulk μ' and dynamic μ viscosities[58], with $\beta = \frac{\mu'}{\mu} + \frac{1}{3}$. The equation of state formulates the constitutive relation between density, pressure, and temperature, with

$$\rho_1 = \frac{p_1}{c_w^2} - \rho_{0,w}\alpha T_1, \tag{S13}$$

where c_w is the sound speed.

At the solid-fluid boundary, the velocity is set to be continuous, with

$$v_1 = -i\omega u_1, \tag{S14}$$

additionally, a slip boundary condition is enforced along the sides and walls of the fluid domains, ensuring that:

$$v_1 \cdot n = 0. \tag{S15}$$

Adiabatic boundary conditions on the fluid domain boundaries then complete the numerical model, with

$$n \cdot \left(D_T \nabla T_1\right) = 0. \tag{S16}$$

To excite the acoustic field in the simulation domain, a harmonic excitation is applied at the bottom boundary:

$$i\omega u_{1,z} = v_{1,z} = 0.1(m/s). \tag{S17}$$

This boundary condition models the domain actuation with a bulk-wave piezoelectric actuator used in the experiment.
As the Navier–Stokes governing equations are non-linear, the harmonic actuation generates higher-order responses. Following perturbation theory, the second-order time-averaged fields in the fluid domain $\langle g_2(r,t)\rangle$ can be determined, with

$$-\nabla\cdot\langle\rho_1 v_1\rangle = \rho_0\nabla\cdot v_2, \tag{S18}$$

$$\rho_0\langle(v_1\cdot\nabla)v_1\rangle + \left\langle\rho_1\frac{\partial v_1}{\partial t}\right\rangle = -\nabla\langle p_2\rangle + \beta\mu\nabla(\nabla\cdot v_2) + \mu\nabla^2 v_2. \tag{S19}$$

Hence, the first-order fields drive the second-order steady flow field v_2, termed acoustic streaming. To appropriately model the interaction of flowing fluid with structures, non-slip boundary conditions are applied at fluid-solid interfaces, with

$$v_2 = 0, \tag{S20}$$

and a slip boundary condition (symmetry condition) on the outer side walls (in the fluid domain), with

$$v_2\cdot n = 0. \tag{S21}$$

The time-averaged acoustophoretic radiation force on a spherical particle exposed to an acoustic standing wave is then given by Gor'kov[59], with

$$\begin{aligned} &F^{rad} = -\nabla U^{rad},\ U^{rad} = U^{rad}_{mp} + U^{rad}_{dp} = V_{ps}\left(\frac{1}{2}f_1 k_w\langle p_1^2\rangle - \frac{3}{4}f_2\rho_{w,0}\langle v_1^2\rangle\right)\\ &V_{ps} = \frac{\pi}{6}d_{ps}^3,\ f_{mp} = 1-\frac{k_{ps}}{k_w},\ f_{dp} = \frac{2(\rho_{ps}-\rho_{0,w})}{2\rho_{ps}+\rho_{0,w}},\ k_w = \frac{1}{\rho_{w,0}c_w^2}, \end{aligned} \tag{S22}$$

where U_{rad} is the Gor'kov time-averaged potential, superscripts *mp* and *dp* denote monopole and dipole terms, V_{ps} is a particle volume, k is compressibility, ρ is density, superscripts w and ps denote water and polystyrene beads respectively, $\langle AB\rangle = 0.5Re(A^* B)$ is the time average over one oscillation period of complex time-harmonic fields A and B, the asterisk denotes complex conjugation, d_{ps} is particle diameter. The Eq. (S22) is valid for particles with a diameter below the Rayleigh scattering limit $d_{ps} \ll \lambda = 213\mu m$ at 7 MHz.

Unlike the acoustophoretic force exerted by the harmonic fields, steady acoustic streaming applies a viscous drag force on particles suspended in a fluid. By implying zero background flow $v_0 = 0$, the fluid drag force on a spherical particle caused by the streaming flow can be written as follows:

$$F^{drag} = 3\pi\mu d_{ps}(v_2 - v_{ps}), \tag{S23}$$

where v_{ps} is the particle velocity.

Supplementary Note 3
Mesh study

A hybrid computational mesh was used in the study as shown in Fig. S3b-e. To ensure that mesh refining does not change the solution significantly, a mesh convergence analysis was conducted using the approach from Devendran et al.[62] and Muller et al.[40]. A convergence function $C(g)$ over the interior of Ω (Fig. S3e) can be written as follows, with

$$C(g) = \sqrt{\frac{\int_{\Omega} \left(U_{g}^{rad} - U_{ref}^{rad}\right)^2 dr\, dz}{\int_{\Omega} \left(U_{ref}^{rad}\right)^2 dr\, dz}}, \tag{S24}$$

where g is the current solution and U_{ref}^{rad} is a reference solution. Current and reference solutions have a maximum mesh element size of d_m and $d_{m,ref} = 3\ \mu m$ respectively. The fluid domain has mesh refinement near the boundary layer. The mesh study was performed for a $w = 30\ \mu m$, $h = 70\ \mu m$, $\alpha = 13°$ microstructure. Fig. S3f shows Gor'kov potential convergence in the fluid domain. A convergence threshold of $C(g) < 0.001$ is realized in a computational mesh with $d_m = 6$ μm used in this study.

The modeling domain dimensions can potentially affect the solution in the vicinity of the structure due to edge effects. To estimate the minimum domain radius R which does not have any substantial impact on the solution a parametric study was converted. Fig. S3g plots the convergence function $C(R)$ (S24) for the computational domains of various sizes. The function $C(R)$ was evaluated in the fixed-sized Ω subdomain as denoted in Fig. S3e. The reference solution is taken for a large domain with $R = 400\ \mu m$. The function rapidly converges and doesn't exceed 2% beyond $200\ \mu m$, hence a $R = 200\ \mu m$ domain was selected for further study.

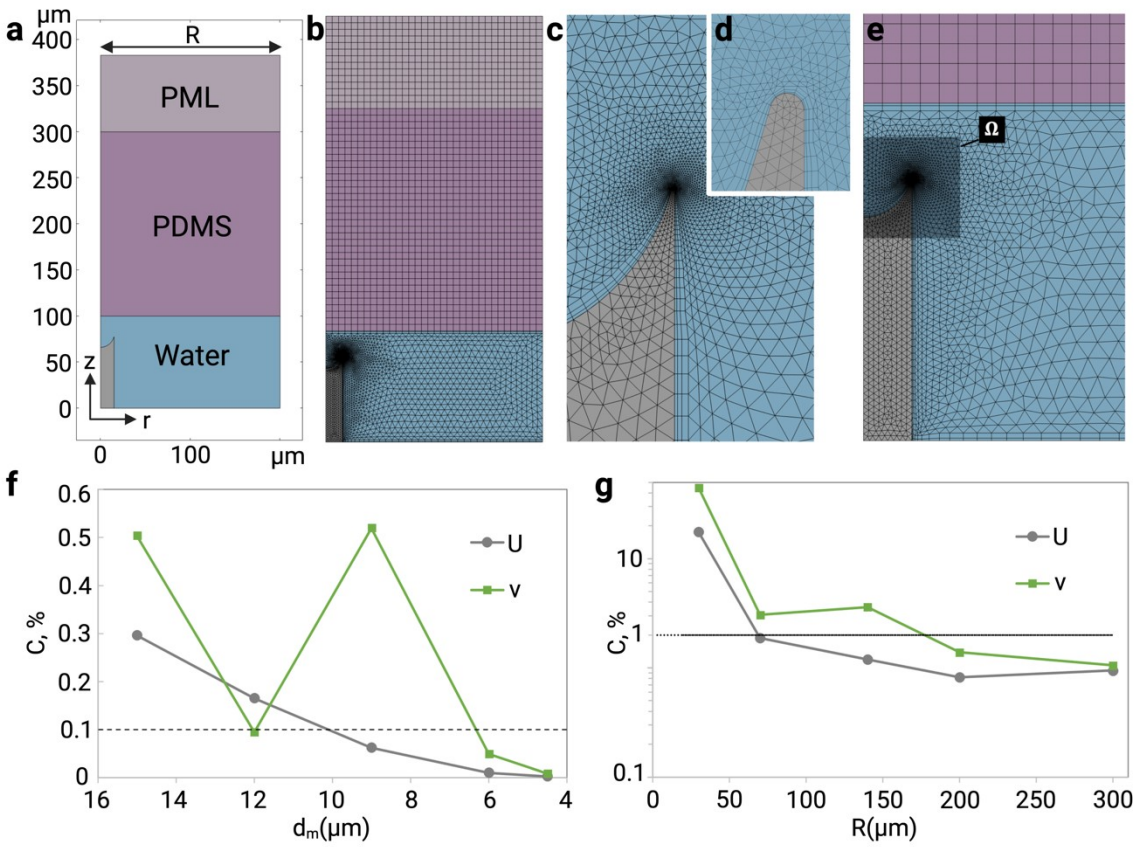

Fig. S3. Numerical modeling set-up. (a) Modeling domain in cylindrical coordinates (b-e) where (b) shows the computational grid for the study. (c) Close-up of the computational mesh for the fluid domain, with (d) showing the mesh elements at the fluid/solid boundary. (e) The study subdomain Ω for the mesh and domain size analysis. (f) Mesh convergence study for the Gor'kov potential U_{rad} field and acoustic streaming velocity magnitude field. The dashed line indicates $C = 0.001$ threshold. (g) Effect of the computational domain radius R on the Gor'kov potential U_{rad} value and acoustic streaming velocity magnitude field. The dotted line indicates $C = 0.02$ threshold.

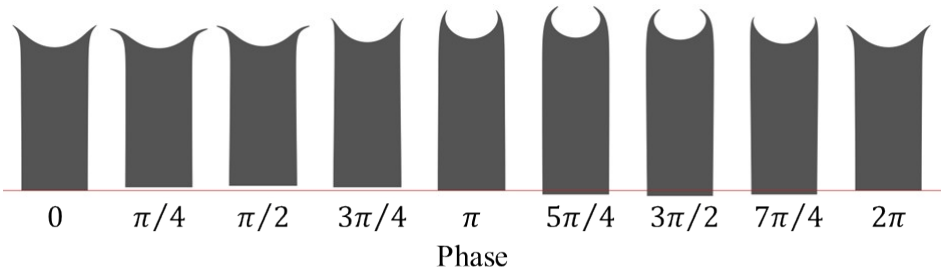

Fig. S4. Time evolution of the sharp edge structure shape ($\alpha = 13°$) actuated at 7 MHz. The deformation is scaled up 100 times for visualization.

Table S1. Material properties used in the computational study.

Material / Property	**Notation**	**Value**
Polydimethylsiloxane (PDMS)[63, 64]		
Density	$\rho_{0,p}$	1070 kg m^{-3}
Longitudinal wave speed	$c_{L,\,p}$	1030 m s^{-1}
Transverse (shear) wave speed	$c_{T,\,p}$	100 m s^{-1}
Loss factor	η_p	0.001
Water [62]		
Density	$\rho_{0,w}$	997 kg m^{-3}
Sound speed	c_w	1497 m s^{-1}
Dynamic viscosity	μ	0.00089 Pa s
Bulk viscosity	μ'	0.00247 Pa s
Viscous boundary layer	$\delta_v = \sqrt{2\mu/\rho\omega}$	0.2 µm
Thermal conductivity	D_T	0.603 W m^{-1} K^{-1}
Specific heat capacity	C_p	4183 J kg^{-1} K^{-1}
Thermal expansion coefficient	α_T	0.000297 K^{-1}
IP-Dip		
Density[65]	$\rho_{0,s}$	1170 kg m^{-3}
Young's Modulus[66]	E_s	2.91 GPa
Poisson ratio[67]	ν_s	0.3
Loss factor[68]	η_s	0.023
Polystyrene beads[69]		
Density	ρ_{ps}	1050 kg m^{-3}
Compressibility	k_{ps}	249 TPa^{-1}
Diameter	d_{ps}	1 µm